

# Co(II) Schiff Base Complexes Encapsulated in the Nanopores of Zeolite Y as Heterogeneous Catalysts for Selective Epoxidation of Alkenes with Molecular Oxygen

B. Rezazadeh<sup>a</sup>, A. R. Pourali<sup>a, \*</sup>, A. R. Banaei<sup>b, \*\*</sup>, and S. Tabari<sup>a</sup>

<sup>a</sup> School of Chemistry, Damghan University, Damghan, Iran

<sup>b</sup> Department of Chemistry, Payame Noor University, Tehran, Iran

\*e-mail: pourali@du.ac.ir

\*\*e-mail: banaei@pnu.ac.ir

Received May 15, 2020; revised June 21, 2020; accepted July 2, 2020

**Abstract**—Co(II) macrocyclic Schiff base complex nanoparticles have been encapsulated in the nanopores of zeolite Y. The new Schiff base complexes entrapped in the nanoreactor of zeolite Y were characterized by several techniques: chemical analysis and spectroscopic methods (FT-IR, XRD, and DRS). These complexes (neat and encapsulated) were used for epoxidation of alkenes with O<sub>2</sub> as oxidant in different solvents. The catalyst demonstrated excellent activity for a variety of alkenes in a mild, inexpensive and efficient protocol. Reaction parameters including temperature, catalyst amount and solvent were screened by reaction time. The recycling experiment results indicated that the catalysts were highly stable and maintained activity and selectivity even after being used for five cycles.

**Keywords:** nanoporous material, epoxidation of alkenes, cobalt(II) Schiff base complex, heterogeneous catalyst, zeolite Y encapsulated complex

**DOI:** 10.1134/S107032842106004X

## INTRODUCTION

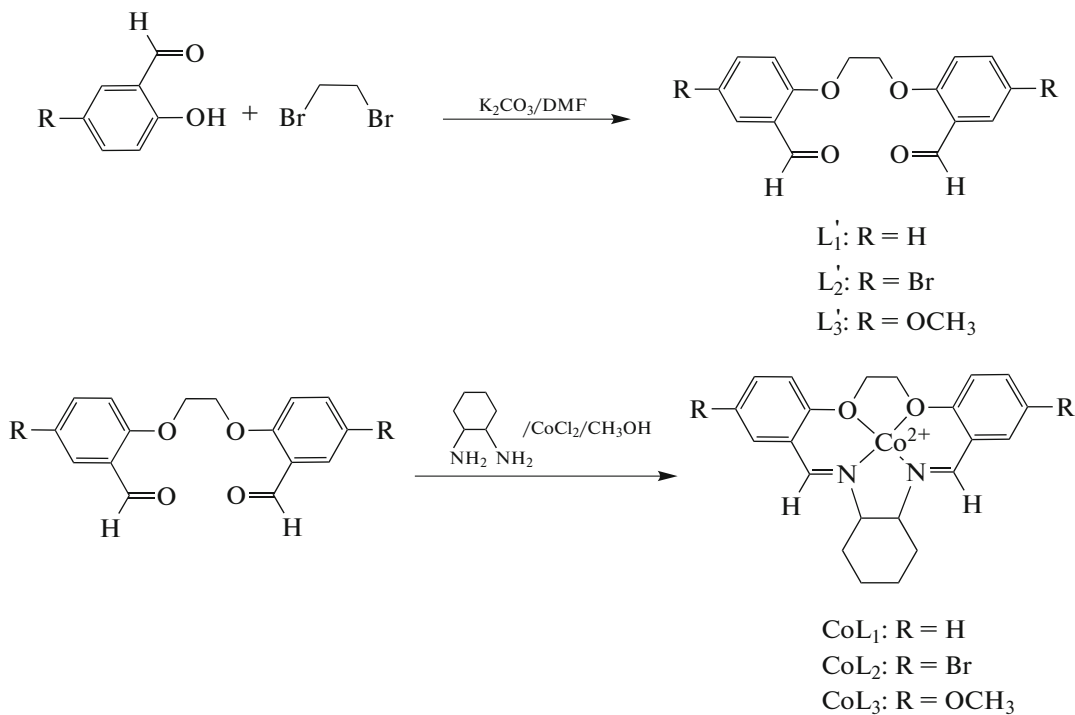
Oxidation of hydrocarbons is of great interest in synthetic organic chemistry and chemical industry for the conversion of petroleum-based feedstock to more valuable chemicals, such as epoxides, diols, alcohols and carbonyl compounds [1]. Among such oxidation reactions, the epoxidation of alkenes represents a comfortable way to activate and functionalize them which quite often serves as the first stage of various kinds of industrial production [2, 3]. Among various oxidants, molecular oxygen is a clean, cheap and readily available oxidant, making it ideal for hydrocarbon oxidation from both environmental and economic viewpoints [4]. Recently, attention has been focused on metal–Schiff base complexes for aerobic oxidation of olefins [5]. Co complexes are known as efficient catalysis for the epoxidation of olefins [6], and the potential of Co complexes for the aerobic epoxidation of olefins has been known for decades [7]. Cobalt ions and their coordination complexes catalyze the selective oxidation of olefins and alkylbenzenes with O<sub>2</sub> [8]. Cobalt complexes are also used in the epoxidation of alkenes with *tert*-butyl hydroperoxide (TBHP) and iodosylbenzene [9]. The catalytic oxidation of termi-

nal olefins, including styrene, by O<sub>2</sub> to the corresponding 2-ketones and 2-alcohols using a cobalt(II) complex has been reported [10]. Cobalt–salen complexes were reported to show catalytic activity for the epoxidation of styrene with O<sub>2</sub> in the presence of a co-reductant, isobutyraldehyde [11].

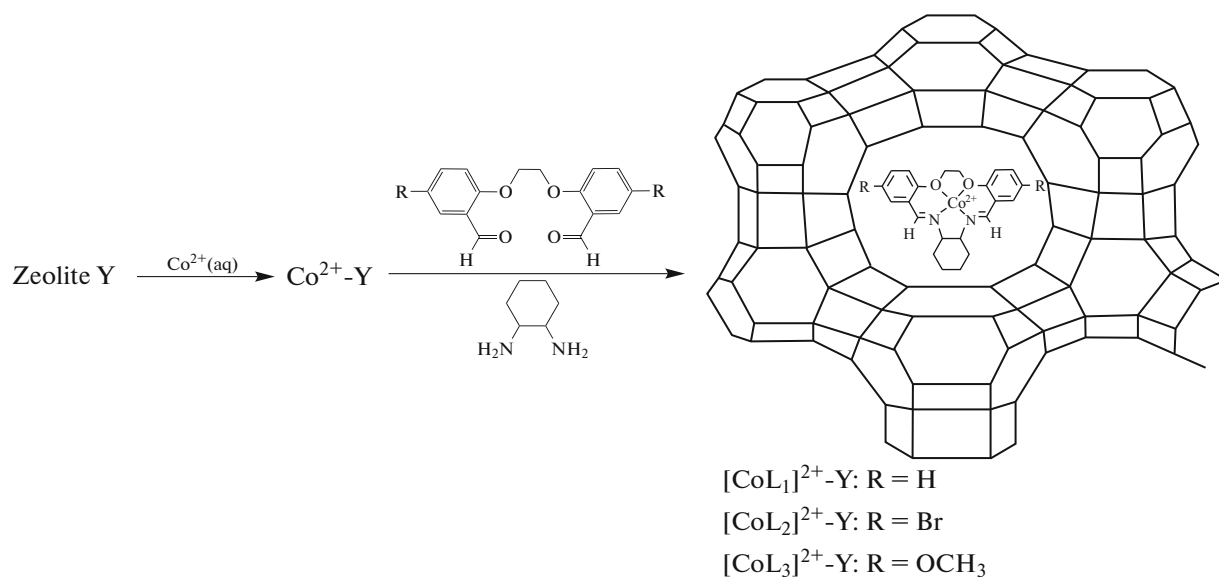
However, most of such epoxidation reactions are still using homogeneous catalysts. From the sustainable and green chemistry point of view, heterogeneous catalysts would be interesting since they offer the benefits of possible catalyst recycle, easy catalyst separation and sometimes high selectivity and activity [12]. In this respect, encapsulation of transition metal complex in zeolite Y gained much interest in the last decade [13]. Since this process can lead to the materials with both homogeneous catalysis and heterogeneous catalysis characters. Also, dimerization of the transition metal complexes and degradation of the ligands could occur during homogeneous catalysis reactions, resulting in a reduction in the activity, and even irreversible deactivation. In contrast, upon encapsulation in zeolites Y, transition metal complex molecules are engaged and site-isolated, making these complexes stable, highly active and selective for the epoxidation of olefins. Recently, we have reported for synthesis of Cu(II) macrocyclic Schiff

base complexes inside zeolite Y. Cu(II) Schiff base complexes were found to be efficient catalyst for epoxidation of cyclooctene [14]. Looking into the advantage of zeolite Y encapsulated Schiff base complexes, in this study we report the synthesis and characterization of the new Co(II) macrocyclic Schiff

base complexes ( $\text{CoL}_1\text{Cl}_2$ ,  $\text{CoL}_2\text{Cl}_2$  and  $\text{CoL}_3\text{Cl}_2$ ) inside zeolite Y. Synthesis of  $\text{CoL}_1\text{Cl}_2$ ,  $\text{CoL}_2\text{Cl}_2$  and  $\text{CoL}_3\text{Cl}_2$  complexes is given in Scheme 1, and synthesis of  $[\text{CoL}_1]^{2+}\text{-Y}$ ,  $[\text{CoL}_2]^{2+}\text{-Y}$  and  $[\text{CoL}_3]^{2+}\text{-Y}$  is given in Scheme 2.



Scheme 1.



Scheme 2.

## EXPERIMENTAL

**Materials and physical measurements.** All materials were purchased from Sigma Aldrich and Merck and used as received without any purification. FT-IR spectra were recorded on Shimadzu Varian 4300 spectrophotometer in KBr pellets. Diffuse reflectance spectra (DRS) were registered on a Scinco 4100 the range 200–1100 nm using 6890 series. The elemental analysis (C, H and N) of the materials was obtained from Carlo ERBA model EA 1108 analyzer. The X-ray diffraction (XRD) patterns were recorded by a Rigaku D-Max C III, X-ray diffractometer using Ni-filtered  $\text{CuK}\alpha$  radiation. The metal contents of the samples were measured by Atomic Absorption Spectrophotometer (AAS) (AAS-Perkin-Elmer 4100-1319) using a flame approach. After completely destroying the zeolitic framework with hot and concentrated HCl, aluminum, sodium and cobalt were analyzed by AAS and  $\text{SiO}_2$  was determined by gravimetric analysis. The  $^1\text{H}$  NMR and  $^{13}\text{C}$  NMR spectra were recorded on a Bruker Asend TM 400 MHz spectrometer in  $\text{DMSO-d}_6$  and  $\text{CDCl}_3$  using tetramethylsilane (TMS) as an internal reference. Thermal studies were performed on a NETZSCH STA 409 PC/PG in a nitrogen atmosphere with a heating rate of  $20^\circ\text{C}/\text{min}$  in the temperature range of  $25\text{--}750^\circ\text{C}$ . The products were analyzed by gas chromatography (GC) and GC-Mass using 6890 series, FID detector, HP, 5% 5-phenyl siloxane and agilent 5973 network, mass selective detector, HP, 5MS 6890 network GC system.

**Synthesis of  $\text{L}'_1$ .** To stirred solution of salicylaldehyde (50 mmol) and  $\text{K}_2\text{CO}_3$  (3.05 g, 25 mmol) in dimethylformamide (DMF) (75 mL) was added drop wise 1,2-dibromoethane (9.4 g, 50 mmol) in DMF (25 mL). The reaction was continued for 6 h at  $150^\circ\text{C}$  and then 1 h at  $25^\circ\text{C}$ . After that it was completed, 250 mL of distilled water were added and the mixture was put in the refrigerator. After 1 h the precipitate was filtered and washed with 500 mL distilled water, then dried and recrystallized from ethanol and dried in vacuum. The yield was 4.99 g (76%), m.p.  $130^\circ\text{C}$ , color—cream.

For  $\text{C}_{16}\text{H}_{14}\text{O}_4$

Anal. calcd., %	C, 71.11	H, 5.18
Found, %	C, 71.16	H, 5.22

IR (KBr;  $\nu$ ,  $\text{cm}^{-1}$ ): 1675  $\nu(\text{C}=\text{O})$ , 1484, 1468  $\nu(\text{Ar}-\text{C}=\text{C})$ , 1285, 1235  $\nu(\text{Ar}-\text{O})$ , 1173, 1045  $\nu(\text{R}-\text{O})$ .  $^1\text{H}$  NMR ( $\text{DMSO-d}_6$ ; 400 MHz;  $\delta$ , ppm): 10.30 (s., 2H, CHO), 7.65 (d.d., 4H, ArH), 7.33 (d., 2H, ArH), 7.093 (t., 2H, ArH), 4.58 (s., 4H,  $\text{OCH}_2$ ).  $^{13}\text{C}$  NMR ( $\text{DMSO-d}_6$ ; 400 MHz;  $\delta$ , ppm): 189.62, 161.32, 136.88, 128.04, 124.99, 121.61, 114.65, 67.89.

**Synthesis of  $\text{L}'_2$  and  $\text{L}'_3$ .** 5-Bromo-2-hydroxybenzaldehyde or 5-methoxy-2-hydroxybenzaldehyde (50 mmol) was dissolved in 75 mL DMF and  $\text{K}_2\text{CO}_3$  added and mixture was stirred at  $25^\circ\text{C}$  and 1,2-dibromoethane (9.4 g, 25 mmol) was added drop wise and then the reaction mixture was stirred under reflux for 6 h. The resulted mixture was partitioned between water and ethylacetate, the ethyl acetate layer was collected and concentrated under reduced pressure and then subjected to silica gel 100–200 mesh column chromatography using hexane–ethylacetate (1 : 10) as eluent to afford compounds in pure form.

$\text{L}'_2$ : yield 8.35 g (78%), m.p.  $143^\circ\text{C}$ , color—cream.

For  $\text{C}_{16}\text{H}_{12}\text{O}_4\text{Br}_2$

Anal. calcd., %	C, 44.86	H, 2.80
Found, %	C, 44.91	H, 2.83

IR (KBr;  $\nu$ ,  $\text{cm}^{-1}$ ): 1678  $\nu(\text{C}=\text{O})$ , 1491, 1471  $\nu(\text{Ar}-\text{C}=\text{C})$ , 1289, 1237  $\nu(\text{Ar}-\text{O})$ , 1176, 1049  $\nu(\text{R}-\text{O})$ .  $^1\text{H}$  NMR ( $\text{DMSO-d}_6$ ; 400 MHz;  $\delta$ , ppm): 10.20 (s., 2H, CHO), 7.82 (d.d., 2H, ArH), 7.73 (d., 2H, ArH), 7.33 (d., 2H, ArH), 4.53 (s., 4H,  $\text{OCH}_2$ ).  $^{13}\text{C}$  NMR ( $\text{DMSO-d}_6$ ; 400 MHz;  $\delta$ , ppm): 188.59, 160.29, 138.92, 130.23, 126.52, 117.47, 113.42, 68.21.

$\text{L}'_3$ : yield 5.78 g (70%), m.p.  $118^\circ\text{C}$ , color—cream.

For  $\text{C}_{18}\text{H}_{18}\text{O}_6$

Anal. calcd., %	C, 65.45	H, 5.45
Found, %	C, 65.51	H, 5.48

IR (KBr;  $\nu$ ,  $\text{cm}^{-1}$ ): 1673  $\nu(\text{C}=\text{O})$ , 1495, 1477  $\nu(\text{Ar}-\text{C}=\text{C})$ , 1283, 1234  $\nu(\text{Ar}-\text{O})$ , 1170, 1042  $\nu(\text{R}-\text{O})$ .  $^1\text{H}$  NMR ( $\text{DMSO-d}_6$ ; 400 MHz;  $\delta$ , ppm): 10.52 (s., 2H, CHO), 7.41 (q., 2H, ArH), 7.14 (d., 4H, ArH), 4.50 (s., 4H,  $\text{OCH}_2$ ), 3.88 (s., 6H,  $\text{OCH}_3$ ).  $^{13}\text{C}$  NMR ( $\text{DMSO-d}_6$ ; 400 MHz;  $\delta$ , ppm): 190.54, 152.81, 151.1, 129.99, 124.32, 119.19, 117.93, 73.08, 55.96.

**Synthesis of  $\text{CoL}_1\text{Cl}_2$ ,  $\text{CoL}_2\text{Cl}_2$  and  $\text{CoL}_3\text{Cl}_2$  complexes.** To stirred solution of dialdehyde ligand ( $\text{L}'_1$ ,  $\text{L}'_2$  or  $\text{L}'_3$ ) (12 mmol) and  $\text{CoCl}_2$  (12 mmol, 1.56 g) in methanol (80 mL), *trans*-( $\pm$ )-diaminocyclohexane (12 mmol) in methanol (30 mL) was added drop wise. After the addition was completed the stirring was continued for 1 h. Then the precipitate was filtered and washed with methanol and dried for 24 h at  $100^\circ\text{C}$  under vacuum.

$\text{CoL}_1\text{Cl}_2$ :

For  $\text{C}_{22}\text{H}_{24}\text{O}_2\text{N}_2\text{Cl}_2\text{Co}$

Anal. calcd., %	C, 55.23	H, 5.02	N, 5.85	Co, 12.34	C/N, 9.44
Found, %	C, 55.26	H, 5.05	N, 5.81	Co, 12.32	C/N, 9.50

IR (KBr;  $\nu$ ,  $\text{cm}^{-1}$ ): 1624  $\nu(\text{C}=\text{N})$ , 520  $\nu(\text{Co}-\text{O})$ , 510  $\nu(\text{Co}-\text{N})$ ,  $\Lambda_{\text{M}} = 183 \Omega^{-1} \text{cm}^2 \text{mol}^{-1}$  (in DMF), DRS ( $\lambda_{\text{max}}$ , nm): 297, 315, 363, 470,  $\mu_{\text{eff}} = 3.85 \mu_{\text{B}}$ .

$\text{CoL}_2\text{Cl}_2$ :

For  $\text{C}_{22}\text{H}_{22}\text{O}_2\text{N}_2\text{Cl}_2\text{Br}_2\text{Co}$

Anal. calcd., % C, 41.50 H, 3.46 N, 4.40 Co, 9.27 C/N, 9.43

Found, % C, 41.57 H, 3.51 N, 4.39 Co, 9.23 C/N, 9.47

IR (KBr;  $\nu$ ,  $\text{cm}^{-1}$ ): 1628  $\nu(\text{C}=\text{N})$ , 525  $\nu(\text{Co}-\text{O})$ , 514  $\nu(\text{Co}-\text{N})$ ,  $\Lambda_{\text{M}} = 181 \Omega^{-1} \text{cm}^2 \text{mol}^{-1}$  (in DMF), DRS ( $\lambda_{\text{max}}$ , nm): 297, 314, 360, 466,  $\mu_{\text{eff}} = 3.88 \mu_{\text{B}}$ .

$\text{CoL}_3\text{Cl}_2$ :

For  $\text{C}_{24}\text{H}_{28}\text{O}_4\text{N}_2\text{Cl}_2\text{Co}$

Anal. calcd., % C, 53.53 H, 5.20 N, 5.20 Co, 10.96 C/N, 10.29

Found, % C, 53.59 H, 5.24 N, 5.15 Co, 10.90 C/N, 10.40

IR (KBr;  $\nu$ ,  $\text{cm}^{-1}$ ): 1623  $\nu(\text{C}=\text{N})$ , 522  $\nu(\text{Co}-\text{O})$ , 509  $\nu(\text{Co}-\text{N})$ ,  $\Lambda_{\text{M}} = 180 \Omega^{-1} \text{cm}^2 \text{mol}^{-1}$  (in DMF), DRS ( $\lambda_{\text{max}}$ , nm): 297, 314, 362, 475,  $\mu_{\text{eff}} = 3.84 \mu_{\text{B}}$ .

**Synthesis of Co(II)-Y.** 4 g of zeolite Y was mixed in a round bottom flask with 250 mL of 30 mmol aqueous solution of  $\text{CoCl}_2$  and the resultant mixture was refluxed for 24 h. To prevent metal hydroxide preparation, the pH of the solution was maintained in between 4–5. The solid was filtered and washed with hot distilled water to remove all dissolved chloride ions or until it gives negative test with  $\text{AgNO}_3$ . The Co(II) exchanged zeolite Y were then dried for 12 h in an oven at  $100^\circ\text{C}$  for further use.

Zeolite Y: anal. found, %: Si, 21.76 Al, 8.61 Si/Al: 2.53

Co(II)-Y: anal. found, %: Si, 21.55 Al, 8.51 Na, 4.42 Co, 3.86 Si/Al: 2.53

### Synthesis of zeolite Y encapsulated Co(II) complexes.

Co(II)-Y (2g) and 5 mmol dialdehyde ligand ( $L'_1$ ,  $L'_2$  and  $L'_3$ ) dispersed in 50 mL DMF and excess of *trans*-( $\pm$ )-diaminocyclohexane (0.8 g) in 25 mL DMF was added to this reaction mixture and refluxed for 48 h under  $\text{N}_2$  atmosphere. The change in the color of solid mass after reaction gives preliminary clue about the

formation of complexes inside the supercages of zeolite Y. The solution was filtered and the resulting solids, were soxhelt extracted with diethyl ether (for 3 h) and then with ethanol (for 4 h) to remove extra unreacted products from amine-dialdehyde condensation and any cobalt(II) complexes adsorbed onto the external surface of the zeolite Y crystallites. The resulting powders were dried at  $100^\circ\text{C}$  under vacuum for 12 h.

$[\text{CoL}_1]^{2+}\text{-Y}$ . Anal. found: C, 12.88; H, 1.35; N, 1.37; C/N, 9.40. Si, 21.17; Al, 8.34; Co, 2.88; Si/Al, 2.53. IR (KBr;  $\nu$ ,  $\text{cm}^{-1}$ ): 1618  $\nu(\text{C}=\text{N})$ , DRS ( $\lambda_{\text{max}}$ , nm): 297, 314, 377, 515.

$[\text{CoL}_2]^{2+}\text{-Y}$ . Anal. found: C, 12.52; H, 1.32; N, 1.33; C/N, 9.41. Si, 21.04; Al, 8.32; Co, 2.80; Si/Al, 2.53. IR (KBr;  $\nu$ ,  $\text{cm}^{-1}$ ): 1623  $\nu(\text{C}=\text{N})$ , DRS ( $\lambda_{\text{max}}$ , nm): 297, 314, 387, 520.

$[\text{CoL}_3]^{2+}\text{-Y}$ . Anal. found: C, 13.86; H, 1.51; N, 1.35; C/N, 10.34. Si, 21.12; Al, 8.35; Co, 2.84; Si/Al, 2.53. IR (KBr;  $\nu$ ,  $\text{cm}^{-1}$ ): 1628  $\nu(\text{C}=\text{N})$ , DRS ( $\lambda_{\text{max}}$ , nm): 297, 310, 384, 502.

**Catalytic tests.** Epoxidation of olefins was carried out in a 25-mL three-necked round-bottom flask equipped with  $\text{O}_2$  gas (as an oxidant) inlet (1 atm, bubbling 15 mL/min), water condenser and magnet stirrer bar. In a typical run, a mixture of alkene (10 mmol), isobutyraldehyde (30 mmol) and 20 mg of catalyst ( $[\text{CoL}_1]^{2+}\text{-Y}$ ,  $[\text{CoL}_2]^{2+}\text{-Y}$  or  $[\text{CoL}_3]^{2+}\text{-Y}$ ) were added to acetonitrile (15 mL) and the reaction was kept in a constant temperature oil bath at  $75^\circ\text{C}$ . Molecular oxygen with a rate of  $15 \text{ mL}/\text{min}^{-1}$  was bubbled during the reaction. The reaction mixture was stirred vigorously for a sufficient time. After completion of the reaction, analysis of the oxidation products was determined by gas chromatography with a capillary column and FID detector. Column temperature was programmed between 150 and  $200^\circ\text{C}$  ( $5^\circ\text{C}/\text{min}$ ). Nitrogen was used as carrier gas ( $40 \text{ mL}/\text{min}$ ) at injection temperature.

Activity of the catalyst was expressed as the turnover frequency (TOF) and calculated from the moles of cyclohexene converted per mole of cobalt contained in the catalyst using the following equation:

$$\text{TOF} = \frac{\text{moles (converted cyclooctene)}}{\text{moles of Co (active site)} \times \text{reaction time (h)}}$$

The recovered catalyst which was obtained by simple filtration was washed with  $\text{CH}_3\text{CN}$ , dried at  $100^\circ\text{C}$  for 2 h and then reused for the next run in the same conditions.

## RESULTS AND DISCUSSION

$^1\text{H}$  NMR spectra of  $L'_1$ ,  $L'_2$  recorded in  $\text{DMSO}-d_6$  but spectra of  $L'_3$  recorded in  $\text{CDCl}_3$  (Fig. 1). Aromatic

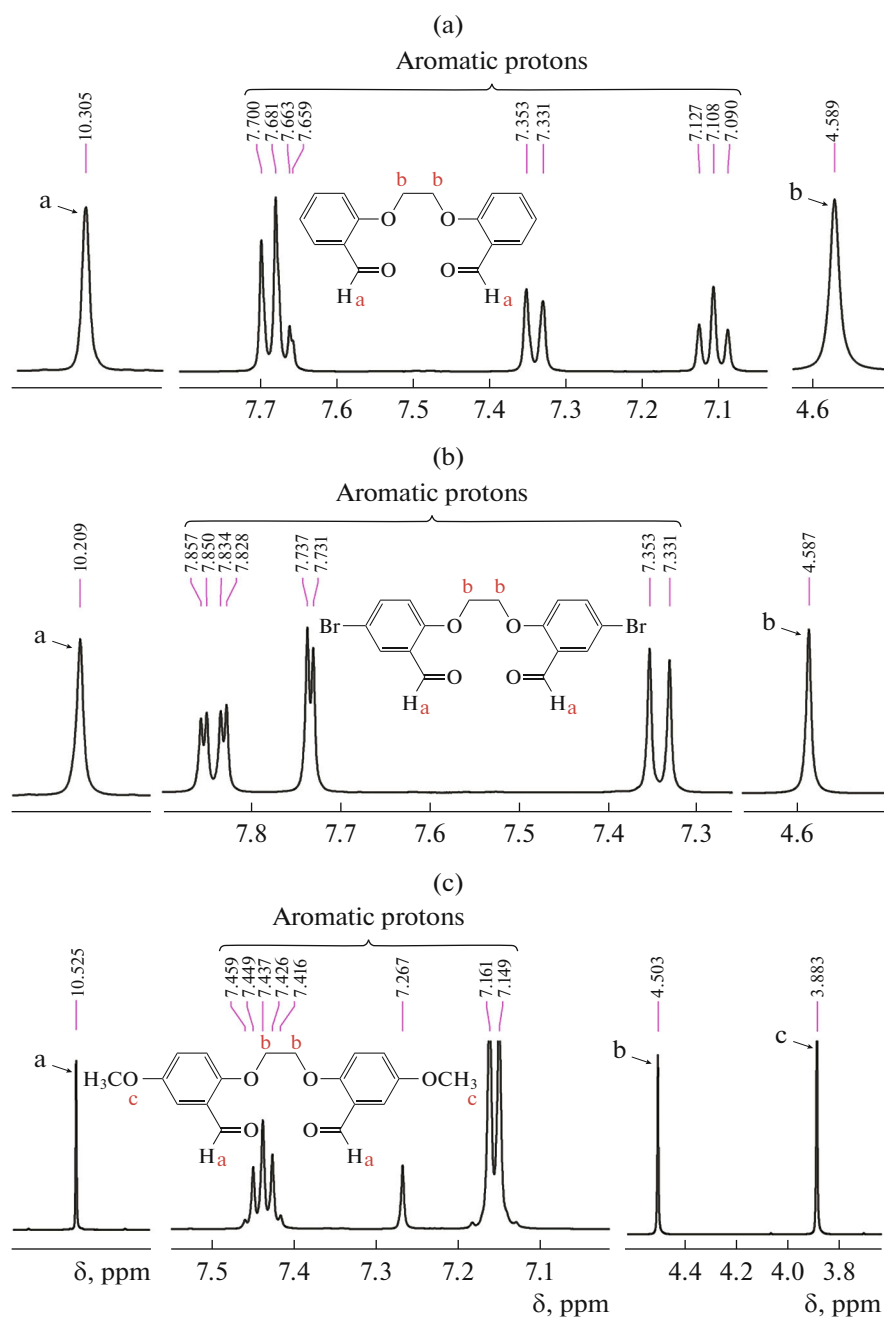
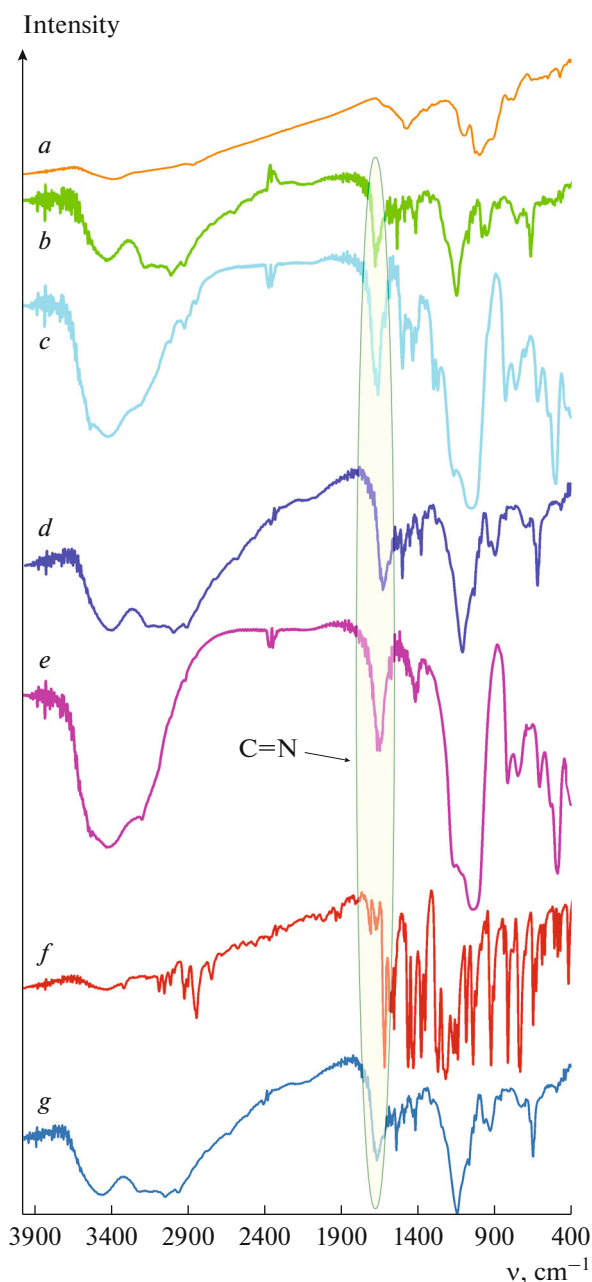


Fig. 1.  $^1\text{H}$  NMR of  $\text{L}'_1$  (a) (recorded in  $\text{DMSO-d}_6$ ),  $\text{L}'_2$  (recorded in  $\text{DMSO-d}_6$ ) (b),  $\text{L}'_3$  (recorded in  $\text{CDCl}_3$ ) (c).

protons were set in the region of 7.09–7.70 ppm for  $\text{L}'_1$ , 7.33–7.85 for  $\text{L}'_2$  and 7.14–7.45 ppm for  $\text{L}'_3$ . Chemical shifts for  $\text{OCH}_2$  and aldehyde protons were found at  $\sim 4.5$  and  $\sim 10.3$  ppm, respectively. Methoxy protons for  $\text{L}'_3$  are represented with a peak at 3.88 ppm.

Zeolite Y encapsulated and neat cobalt Schiff base complexes were initially characterized performing the elemental analyses. The parent zeolite Y has Si/Al

molar ratio of 2.53 which corresponds to a unit cell formula  $\text{Na}_{56}[(\text{AlO}_2)_{56}(\text{SiO}_2)_{136}]$ . Initial cobalt(II) loading in zeolite lattice is 3.86% whereas the metal contents are considerably lower in zeolite Y encapsulated complexes. This decrease in metal contents could be attributed to the formation of complexes inside the zeolite Y cavities. (C, H, N)-Contents in the encapsulated complexes were found to be consistent with the expect molecular formula of the neat com-



**Fig. 2.** FT-IR spectra: zeolite Y (*a*),  $\text{CoL}_1\text{Cl}_2$  (*b*),  $[\text{CoL}_1]^{2+}\text{-Y}$  (*c*),  $\text{CoL}_2\text{Cl}_2$  (*d*),  $[\text{CoL}_2]^{2+}\text{-Y}$  (*e*),  $\text{CoL}_3\text{Cl}_2$  (*f*) and  $[\text{CoL}_3]^{2+}\text{-Y}$  (*g*).

plexes. In particular the C/N ratios in all the zeolite Y encapsulated Co(II) complexes were found to be approximately same as that in the neat Co(II) complexes. The analytical data of each complex indicate molar ratios of Co : C : H almost close to those calculated for the mononuclear structure.

FTIR spectra of neat Co(II) complexes shown in Figs. 2, *b*, *d*, *f* exhibited the characteristic C=N, C=C, C–O stretching vibrations in the region of 1600–1620,

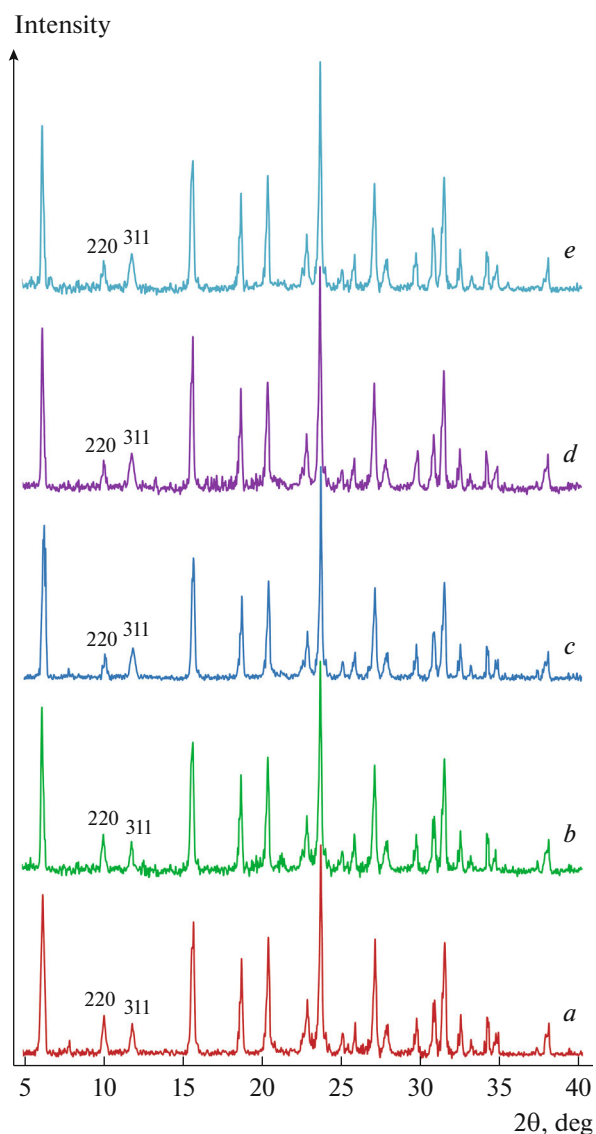


**Fig. 3.** XRD patterns of zeolite Y (*a*), Co(II)-Y (*b*),  $[\text{CoL}_1]^{2+}\text{-Y}$  (*c*),  $[\text{CoL}_2]^{2+}\text{-Y}$  (*d*) and  $[\text{CoL}_3]^{2+}\text{-Y}$  (*e*).

1440–1540 and 1380–1382  $\text{cm}^{-1}$ , respectively [15]. Conclusive, evidence of the bonding is also shown by the observation that new bands in the IR spectra of the neat Co(II) complexes appear at 520 and 510  $\text{cm}^{-1}$  assigned to (Co–O) and (Co–N) stretching vibrations [16]. FT-IR spectrum of zeolite Y (Fig. 2, *a*) shows strong broad band at 1100  $\text{cm}^{-1}$  due to asymmetric stretching vibration of  $(\text{Si}/\text{Al})\text{O}_4$  units [17]. Broad band at 3350  $\text{cm}^{-1}$  can be attributed to stretching vibrations of water and the surface hydroxyl groups of zeolite Y. In the encapsulated complexes, we obtained the similar vibrational band as in the neat Co(II) complexes. In usual case, zeolite Y did not show any bands in the region of 1250–1550  $\text{cm}^{-1}$ . Presence of band in between 1250–1550  $\text{cm}^{-1}$  in the zeolite Y encapsulated complexes also gives a signal for the formation of

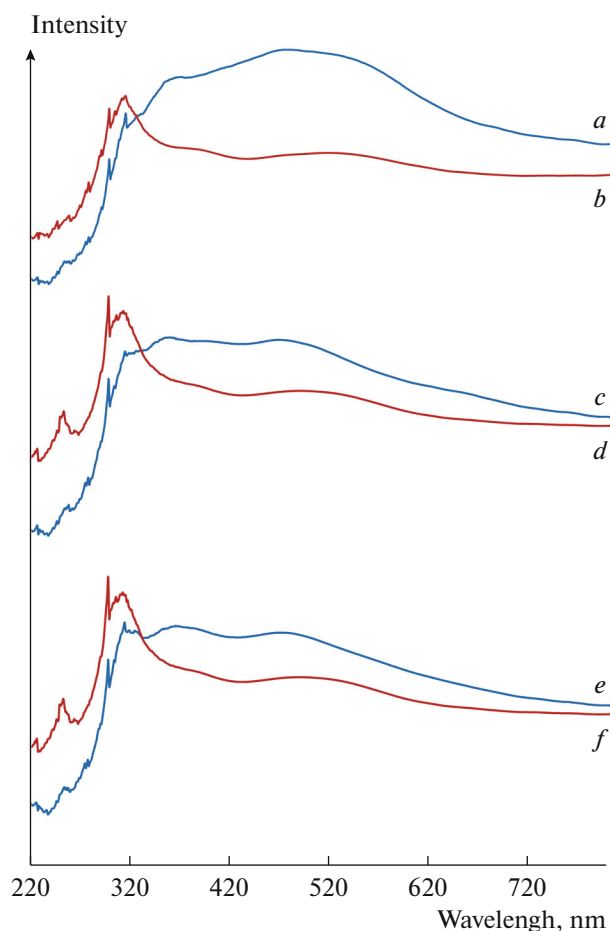


Fig. 4. DRS spectra of  $\text{CoL}_1\text{Cl}_2$  (a),  $[\text{CoL}_1]^{2+}\text{-Y}$  (b),  $\text{CoL}_2\text{Cl}_2$  (c),  $[\text{CoL}_2]^{2+}\text{-Y}$  (d),  $\text{CoL}_3\text{Cl}_2$  (e) and  $[\text{CoL}_3]^{2+}\text{-Y}$  (f).

$[\text{CoL}_1]^{2+}\text{-Y}$ ,  $[\text{CoL}_2]^{2+}\text{-Y}$  and  $[\text{CoL}_3]^{2+}\text{-Y}$ . The IR spectrum of encapsulated complexes show major bands at  $2980$  and  $1635\text{ cm}^{-1}$  which are absent in the zeolite Y. A comparison of the FT-IR spectra of the encapsulated complex with that of the neat complex indicates the presence of the complex inside the zeolite Y cage.

XRD patterns of zeolite Y,  $\text{Co(II)-Y}$  and encapsulated complexes are shown in Fig. 3. The encapsulated complexes exhibit similar peaks to those of zeolite Y, except for a slight change in the intensity of the peaks, no new crystalline pattern emerges. These facts approved that the framework and crystallinity of zeolite Y were not destroyed during the preparation, and that the complexes were well distributed in the cages. The relative peak intensities of the 220 and 311 reflections have been thought to be correlated to the locations of cations. In zeolite Y, the order of peak intensity is in the order:  $I_{220} > I_{311}$ , while in encapsulated complexes, the order of peak intensity became  $I_{311} > I_{220}$ . The difference indicates that the ion-exchanged  $\text{Co}^{2+}$ , which substitutes at the location of  $\text{Na}^+$ , undergoes rearrangement during complexation [18].

The overall geometries of all complexes have been inferred on the basis of the observed values of the magnetic moments. Since all of the  $\text{Co(II)}$  complexes are paramagnetic, their NMR spectra could not be acquired. Magnetic susceptibility measurements give adequate data to characterize the structure of the metal complexes. The magnetic moments of the  $\text{Co(II)}$  complexes performed at room temperature are in the range  $3.84\text{--}3.88\ \mu_{\text{B}}$ , which are characteristic for mononuclear  $\text{Co(II)}$  complexes with a  $S = 3/2$  spin-state and do not signify anti-ferromagnetic coupling of spins at this temperature. The  $\text{Co(II)}$  complexes are 2 : 1 electrolytes as shown by their molar conductivities ( $\Lambda_{\text{M}}$ ) in DMF at  $10^{-3}\text{ M}$ , which are in the range  $180\text{--}183\ \Omega^{-1}\text{ cm}^2\text{ mol}^{-1}$ . The molar conductivities of the compounds in DMF are the range reported for 2 : 1 electrolytes [19, 20].

Solid state UV-Vis electronic absorption spectra of the complexes in neat and encapsulated states are recorded (Fig. 4). The electronic spectra of  $\text{Co(II)}$  complexes exhibit absorption bands at 297, 314 and 365 nm because of the intra ligand  $\pi \rightarrow \pi^*$  transitions and  $n \rightarrow \pi^*$  transitions of azomethine ( $\text{C}=\text{N}$ ) groups,

respectively [21]. They show a broad visible band centered at 470 nm, assigned attributed to the  $d-d$  transitions, characteristic for tetrahedral geometry [22]. The DRS spectra of the encapsulated complexes are shown in Fig. 4, *b, d, f*). They exhibit three characteristic bands at 297, 314 and 380 nm due to  $\pi \rightarrow \pi^*$  and  $n \rightarrow \pi^*$  transitions, respectively, and a broad band centered at 500–520 nm due to  $d-d$  transitions. The comparative UV–Vis spectra of neat complexes and zeolite Y encapsulated metal complexes approved the incorporation of Co(II) complexes into the zeolite Y nanopores.

The TG curves of neat and encapsulated complexes were obtained in a nitrogen atmosphere and are shown in Fig. 5, *a–f*). The TG curve of  $\text{CoL}_1\text{Cl}_2$  and  $\text{CoL}_3\text{Cl}_2$  undergoes decomposition in two stages. The first stage arises in the temperature ranges of 120–260°C with the mass loss of 13% (calcd. 14.9%) in  $\text{CoL}_1\text{Cl}_2$  and 16% (calcd. 13.25%) in  $\text{CoL}_3\text{Cl}_2$  due to the removal of the coordinated counter ions. In the second stage,  $\text{CoL}_1\text{Cl}_2$  and  $\text{CoL}_3\text{Cl}_2$  decompose within the temperature range of 320–550°C with the weight loss of about 30% (calcd. 44.3%) and 40% (calcd. 53.4%), respectively, which is ascribed to the removal of chelating ligands via complex decomposition. As shown in Fig. 5, *c*), complex  $\text{CoL}_2\text{Cl}_2$  displays weight loss of about 65% (calcd. 79%) in the first stage (200–240°C) and 12% (calcd. 11.1%) in the second stage (300–390°C) due to elimination of chelating ligand and coordinated counter ions, respectively.

In case the of zeolite Y encapsulated complexes, the thermal decomposition mainly occurs in the temperature range of 50 to 400°C due to the abstraction of physically and chemisorbed water molecules (about 10%) from the zeolite Y framework [23]. As shown in Fig. 5, *b, d, f*), the encapsulated complexes exhibit a thermal decomposition stage of about 10% beyond 450°C. This minor weight loss can be recognized the existence of only trivial amounts of the Co(II) complex inside the supercages of zeolite Y, which is in an agreement with the low percent Co(II) content measured by the AAS. Moreover, the weight loss due to trapped complex is prolonged (up to 450°C) compared to respective homogeneous counterparts. This observation indicates that the thermal stability of the complexes is considerably enriched upon its encapsulation into zeolite Y supercages. Moreover, the TG curves of the encapsulated complexes show a residual mass of around 75%, clearly suggesting and showing the thermal stability of the composites.

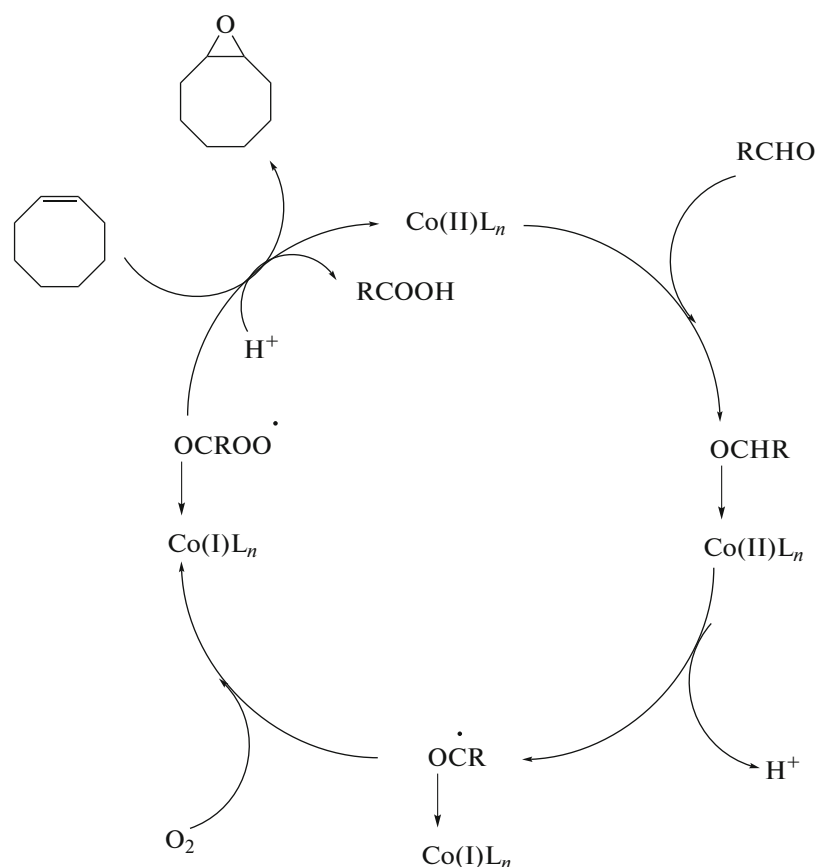
The influence of reaction parameters has been thoroughly examined on the epoxidation of cyclooctene. The catalyst amount, temperature and solvent affected epoxide selectivity and conversion of the reactions and the corresponding results are shown in Table 1. The solvent plays an important role in an oxidation reaction [24]. High possible epoxide selectivity

(88%) and conversion (89%) were obtained in acetonitrile as solvent. Other tested solvents (MeOH, EtOH, and  $\text{CHCl}_3$ ) did not show a good performance compared to acetonitrile (Table 1, entries 1–4, 14–17 and 27–30). The catalyst amount had an impressive role in the progress of the reaction. In the absence of catalyst, the oxidation of cyclooctene by  $\text{O}_2$ /isobutyraldehyde in  $\text{CH}_3\text{CN}$  occurs only up to 8% after 5 h at 75°C. The results on Table 1 (entries 1, 5–7, 14, 18–20, 27 and 31–33) show that increasing the amount of different catalysts up to 20 mg, increased the yield of cyclooctene epoxide. Increasing the temperature to 75°C enhanced the cyclooctene conversion, and the conversion increased almost proportionally with increasing temperature (Table 1, entries 1, 11–13, 14, 24–26, 27 and 37–39). No more conversion could be obtained at a temperature higher than 75°C. We also investigate the reaction progress of the related homogeneous catalysts (Table 1, entries 40–42). Compared with analogous homogeneous catalysts, the heterogeneous catalysts show higher conversion. The higher activity of encapsulated Co(II) complexes is because of site isolation of the complexes. The encapsulation of complexes in zeolites is found to increase the life of the catalyst by preventing the formation of  $\mu$ -oxo,  $\mu$ -peroxo dimeric or other polymeric species due to the restriction of internal framework structure [25].

These new catalysts,  $[\text{CoL}_1]^{2+}\text{-Y}$ ,  $[\text{CoL}_2]^{2+}\text{-Y}$  and  $[\text{CoL}_3]^{2+}\text{-Y}$ , can also be used for the epoxidation of a wide range of substituted olefins (Table 2). Among the endocyclic olefins, cyclooctene were the most reactive of all (Table 2, entry 2). This reactivity arises from the stability of cyclooctene as well as the high reactivity of its double bond [26]. The potential of active allylic hydrogens to oxidation was responsible for diminishing the epoxide selectivity for cyclohexene (Table 2, entry 1). Open-chain olefins, such as 1-octene (Table 2, entry 4) and styrene (Table 2, entry 3) are epoxidized with moderate efficiency. Steric hindrance on the  $\text{C}=\text{C}$  bond not only decreased the conversion of the olefins, such as 1-methoxy-2-methylprop-1-ene (Table 2, entry 5) and 3, 3-dimethylhex-1-ene (Table 2, entry 6) but also increased the reaction time.

According to the reported mechanisms in the literature for cobalt complexes catalyzed epoxidation [26–28] along with our observations, we propose a mechanism for the macrocyclic Schiff base Co(II) complexes-catalyzed epoxidation of olefins with  $[\text{CoL}_1]^{2+}\text{-Y}$ ,  $[\text{CoL}_2]^{2+}\text{-Y}$  and  $[\text{CoL}_3]^{2+}\text{-Y}$  (Scheme 3).





In this mechanism, isopropylacyl radical produced through the electron transfer to the resultant metal complex affords the corresponding oxo-metal-complex radical, which is converted to peroxide-metal-complex radical in reaction with molecular oxygen. A radical chain reaction leads to epoxide. In order to

demonstrate the presence of radical species ( $\downarrow$   $\text{OCROO}\cdot$ )  $\text{Co(I)L}_n$ )

in our reactions, hydroquinone, as a radical scavenger, was added after 1 h of the reaction, and the reaction progress was monitored by GC. It was observed that the reaction stopped immediately upon addition of the radical scavenger (Fig. 6, *b*), which suggests that the

process indeed proceeds via formation of ( $\downarrow$   $\text{OCROO}\cdot$ ) spe-  $\text{Co(I)L}_n$

cies. The results revealed that cyclooctene conversion decreased to almost zero after addition of a small amount of hydroquinone confirming the radical nature of the active oxygen species formed by molecular oxygen with cobalt(II) in the presence of isobutyraldehyde.

The reusability of solid supported catalysts is one of their most important benefits. Therefore, the reusabil-

ity of  $[\text{CoL}_1]^{2+}\text{-Y}$ ,  $[\text{CoL}_2]^{2+}\text{-Y}$  and  $[\text{CoL}_3]^{2+}\text{-Y}$  catalysts were monitored by means of multiple sequential epoxidations of cyclooctene (Table 3). After the reaction, the solid catalyst could be easily recovered from the reaction mixture by simple filtration and is ready for reuse after washing with  $\text{CH}_3\text{CN}$  and drying at  $100^\circ\text{C}$ . It is clear that all heterogeneous catalysts show good reusability without significant loss of selectivity after five times of reusing. In contrast, the neat complexes were totally destroyed during the first run and changed color.

In order to determine the effect of ligands on the epoxidation reaction,  $\text{CoCl}_2$  and zeolite Y were used as catalyst in the similar conditions (Table 1, entries 43 and 44). The results showed that in the absence of ligands the reaction efficiency was very low. In the neat and encapsulated form,  $\text{CoL}_2\text{Cl}_2$  shows maximum reactivity. It is totally evident as the catalytic activity of the complexes is mainly driven by electronic factor of the substituent group present on the phenyl rings [29]. Presence of electron withdrawing group on phenyl rings makes the complex more active as catalyst for the oxidation reaction [30, 31]. In contrary, electron releasing group ( $-\text{OCH}_3$ ) when attached on the phenyl rings, the complex loses its activity to a great range.  $\text{CoL}_3\text{Cl}_2$  complex has more electron density on

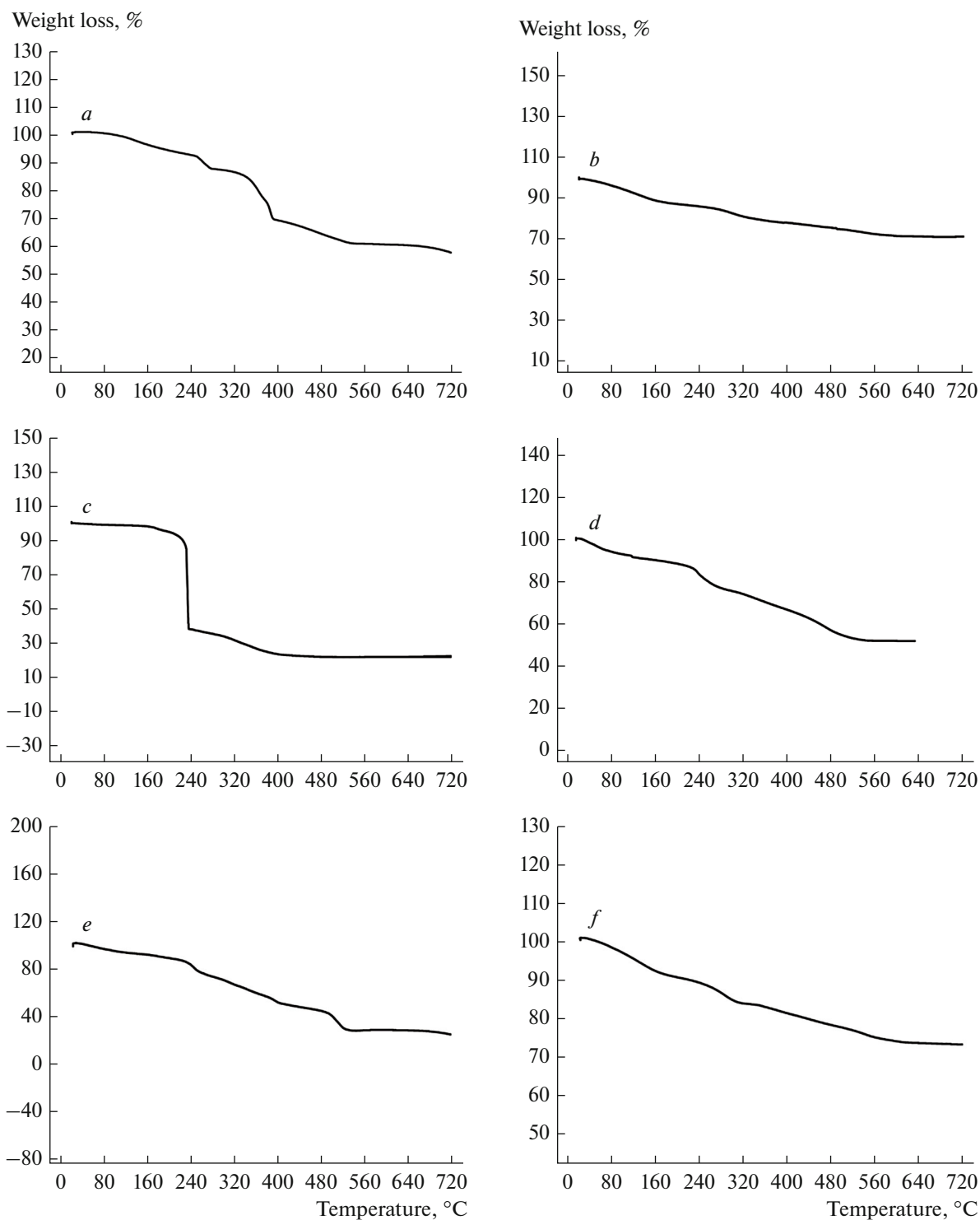


Fig. 5. TGA profiles of  $\text{CoL}_1\text{Cl}_2$  (a),  $\text{CoL}_2\text{Cl}_2$  (b),  $\text{CoL}_3\text{Cl}_2$  (c),  $[\text{CoL}_1]^{2+}\text{-Y}$  (d),  $[\text{CoL}_2]^{2+}\text{-Y}$  (e), and  $[\text{CoL}_3]^{2+}\text{-Y}$  (f).

the metal center and is relatively less reactive for nucleophilic attack than  $\text{CoL}_2\text{Cl}_2$  and also  $\text{CoL}_1\text{Cl}_2$  complex. Therefore the observed trend of activity of the complexes towards the cyclooctene reaction is just in accordance to the expectation.

Many cobalt complexes have been reported for the catalytic epoxidation of alkenes. However, the catalytic systems which have been prepared in this research are superior to most of the reported catalytic protocols in terms of TOF. Also, the advantage of the present

**Table 1.** Epoxidation of cyclooctene with O<sub>2</sub> catalyzed by zeolite Y encapsulated and neat Co(II) complexes

Entry	Catalyst, mg <sup>a</sup>	Solvent <sup>b</sup>	Time, h	TOF, h <sup>-1 c</sup>	Temperature, °C	Conversion, %	Epoxide selectivity, %
1	[CoL <sub>1</sub> ] <sup>2+</sup> -Y (20)	CH <sub>3</sub> CN	2.5	386	75	94.5	97
2	[CoL <sub>1</sub> ] <sup>2+</sup> -Y (20)	CH <sub>3</sub> OH	2.5	278	Reflux	68	92.5
3	[CoL <sub>1</sub> ] <sup>2+</sup> -Y (20)	EtOH	2.5	282	75	69.2	91
4	[CoL <sub>1</sub> ] <sup>2+</sup> -Y (20)	CHCl <sub>3</sub>	2.5	143	Reflux	35	45.2
5	[CoL <sub>1</sub> ] <sup>2+</sup> -Y (10)	CH <sub>3</sub> CN	2.5	446	75	53.5	48
6	[CoL <sub>1</sub> ] <sup>2+</sup> -Y (15)	CH <sub>3</sub> CN	2.5	414	75	74.6	70.5
7	[CoL <sub>1</sub> ] <sup>2+</sup> -Y (25)	CH <sub>3</sub> CN	2.5	312	75	93.7	97.5
8	[CoL <sub>1</sub> ] <sup>2+</sup> -Y (20)	CH <sub>3</sub> CN	1	394	75	38.6	96.3
9	[CoL <sub>1</sub> ] <sup>2+</sup> -Y (20)	CH <sub>3</sub> CN	2	432	75	84.8	96.9
10	[CoL <sub>1</sub> ] <sup>2+</sup> -Y (20)	CH <sub>3</sub> CN	3	324	75	95.3	97.1
11	[CoL <sub>1</sub> ] <sup>2+</sup> -Y (20)	CH <sub>3</sub> CN	2.5	167	35	41	62.3
12	[CoL <sub>1</sub> ] <sup>2+</sup> -Y (20)	CH <sub>3</sub> CN	2.5	339	55	82.8	88.2
13	[CoL <sub>1</sub> ] <sup>2+</sup> -Y (20)	CH <sub>3</sub> CN	2.5	389	80	95.4	95.2
14	[CoL <sub>2</sub> ] <sup>2+</sup> -Y (20)	CH <sub>3</sub> CN	2.5	418	75	98.2	97.9
15	[CoL <sub>2</sub> ] <sup>2+</sup> -Y (20)	CH <sub>3</sub> OH	2.5	291	Reflux	68.3	90
16	[CoL <sub>2</sub> ] <sup>2+</sup> -Y (20)	EtOH	2.5	285	75	67	91.1
17	[CoL <sub>2</sub> ] <sup>2+</sup> -Y (20)	CHCl <sub>3</sub>	2.5	189	Reflux	44.5	51.4
18	[CoL <sub>2</sub> ] <sup>2+</sup> -Y (10)	CH <sub>3</sub> CN	2.5	468	75	55	52.5
19	[CoL <sub>2</sub> ] <sup>2+</sup> -Y (15)	CH <sub>3</sub> CN	2.5	456	75	80.2	88.6
20	[CoL <sub>2</sub> ] <sup>2+</sup> -Y (25)	CH <sub>3</sub> CN	2.5	334	75	98	98.2
21	[CoL <sub>2</sub> ] <sup>2+</sup> -Y (20)	CH <sub>3</sub> CN	1	450	75	42.3	95.8
22	[CoL <sub>2</sub> ] <sup>2+</sup> -Y (20)	CH <sub>3</sub> CN	2	455	75	85.6	97.7
23	[CoL <sub>2</sub> ] <sup>2+</sup> -Y (20)	CH <sub>3</sub> CN	3	350	75	98.6	98
24	[CoL <sub>2</sub> ] <sup>2+</sup> -Y (20)	CH <sub>3</sub> CN	2.5	170	35	40	55.3
25	[CoL <sub>2</sub> ] <sup>2+</sup> -Y (20)	CH <sub>3</sub> CN	2.5	363	55	85.4	90.3
26	[CoL <sub>2</sub> ] <sup>2+</sup> -Y (20)	CH <sub>3</sub> CN	2.5	419	80	98.5	97
27	[CoL <sub>3</sub> ] <sup>2+</sup> -Y (20)	CH <sub>3</sub> CN	2.5	393	75	92.8	97.2
28	[CoL <sub>3</sub> ] <sup>2+</sup> -Y (20)	CH <sub>3</sub> OH	2.5	298	Reflux	70	90.4
29	[CoL <sub>3</sub> ] <sup>2+</sup> -Y (20)	EtOH	2.5	308	75	72.3	91
30	[CoL <sub>3</sub> ] <sup>2+</sup> -Y (20)	CHCl <sub>3</sub>	2.5	134	Reflux	31.5	43.4
31	[CoL <sub>3</sub> ] <sup>2+</sup> -Y (10)	CH <sub>3</sub> CN	2.5	427	75	51.2	41.5
32	[CoL <sub>3</sub> ] <sup>2+</sup> -Y (15)	CH <sub>3</sub> CN	2.5	403	75	72.5	75
33	[CoL <sub>3</sub> ] <sup>2+</sup> -Y (25)	CH <sub>3</sub> CN	2.5	312	75	93.5	98.1
34	[CoL <sub>3</sub> ] <sup>2+</sup> -Y (20)	CH <sub>3</sub> CN	1	378	75	36.3	95.2
35	[CoL <sub>3</sub> ] <sup>2+</sup> -Y (20)	CH <sub>3</sub> CN	2	423	75	81.2	96.4
36	[CoL <sub>3</sub> ] <sup>2+</sup> -Y (20)	CH <sub>3</sub> CN	3	325	75	93.5	97

**Table 1.** (Contd.)

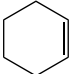
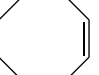
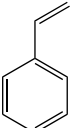
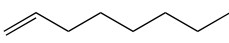
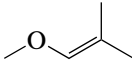
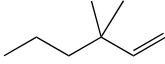
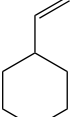
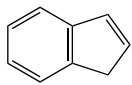
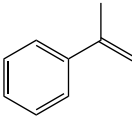
Entry	Catalyst, mg <sup>a</sup>	Solvent <sup>b</sup>	Time, h	TOF, h <sup>-1</sup> <sup>c</sup>	Temperature, °C	Conversion, %	Epoxide selectivity, %
37	[CoL <sub>3</sub> ] <sup>2+</sup> -Y (20)	CH <sub>3</sub> CN	2.5	167	35	40.2	60.4
38	[CoL <sub>3</sub> ] <sup>2+</sup> -Y (20)	CH <sub>3</sub> CN	2.5	340	55	81.7	90.1
39	[CoL <sub>3</sub> ] <sup>2+</sup> -Y (20)	CH <sub>3</sub> CN	2.5	389	80	93.3	97
40	CoL <sub>1</sub> Cl <sub>2</sub> (5)	CH <sub>3</sub> CN	2.5	349	75	90.8	95.8
41	CoL <sub>2</sub> Cl <sub>2</sub> (6)	CH <sub>3</sub> CN	2.5	406	75	95.3	96
42	CoL <sub>3</sub> Cl <sub>2</sub> (5)	CH <sub>3</sub> CN	2.5	375	75	90.1	94.4
43	CoCl <sub>2</sub> (100)	CH <sub>3</sub> CN	2.5		75	23.2	31.6
44	Na-Y (20)	CH <sub>3</sub> CN	2.5		75	13.7	27.3

<sup>a</sup> The amount of metal loadings are 0.49, 0.47, 0.48 (mmol)/g catalyst for [CoL<sub>1</sub>]<sup>2+</sup>-Y, [CoL<sub>2</sub>]<sup>2+</sup>-Y and [CoL<sub>3</sub>]<sup>2+</sup>-Y.

<sup>b</sup> The amount of solvent are 15 mL.

<sup>c</sup> TOF = (mole of reactant)(yield)/(mole of catalyst)(time).

**Table 2.** Epoxidation of some alkenes with O<sub>2</sub> catalyzed by [CoL<sub>1</sub>]<sup>2+</sup>-Y, [CoL<sub>2</sub>]<sup>2+</sup>-Y or [CoL<sub>3</sub>]<sup>2+</sup>-Y. Reaction conditions: alkene (10 mmol), catalyst (20 mg), 75°C, CH<sub>3</sub>CN (15 mL), O<sub>2</sub> (1 atm bubbling 15 mL/min) isobutyraldehyde (30 mmol)

Entry	Alkene	[CoL <sub>1</sub> ] <sup>2+</sup> -Y		[CoL <sub>2</sub> ] <sup>2+</sup> -Y		[CoL <sub>3</sub> ] <sup>2+</sup> -Y	
		conversion (epoxide), %	time, h	conversion (epoxide), %	time, h	conversion (epoxide), %	time, h
1		(90) 86	4	90 (92.5)	4	83.4 (88.2)	4
2		94.5 (97)	2.5	98.2 (97.9)	2.5	92.8 (97.2)	2.5
3		85.2 (93.4)	5	87 (94.8)	5	82.8 (92)	5
4		88.4 (77.5)	8	90.2 (80)	8	86 (75) <sup>a</sup>	8
5		77.4 (81)	12	80 (83.2)	12	75.1 (80)	12
6		78.3 (70)	24	81.5 (71.6)	24	76.6 (69.1) <sup>b</sup>	24
7		84.8 (94.3)	9	86.9 (95.7)	9	80.9 (92.5)	9
8		57.4 (79)	8	59.6 (81.8)	8	55 (77.5) <sup>c</sup>	8
9		88.9 (95.8)	5	92 (96.9)	5	85.7 (94.3)	5

<sup>a</sup> Octanal and octanoic acids were formed as byproducts.

<sup>b</sup> 3,3-Dimethylhexanoic acid, 3,3-dimethylhexanal and 5-hydroxy-2,6,6-trimethylnonan-3-one were formed as byproducts.

<sup>c</sup> 1H-inden-1-ol was formed as a byproduct.

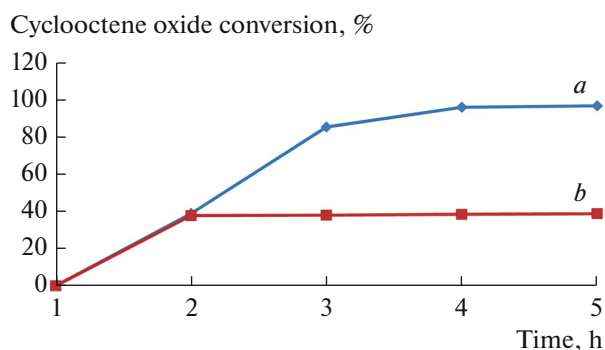


**Fig. 6.** Comparison between reactions without adding a radical scavenger (*a*) and with hydroquinone as a radical scavenger (*b*).

method is that epoxidation happened by these new heterogeneous catalysts in mild conditions by using molecular oxygen as a green oxidant in short reaction times. Very recently, Koner et al. have been immobilized the cobalt(II) Schiff base complex onto the surface of MCM-41, and they have been reported a TOF of 47 [32]. Kazemnejadi et al. have been also decorated

the Co(II)-Schiff base complex onto a polysalicylaldehyde (PSA) framework, and they have been arrived a TOF of 15.4 [33]. Lu et al. have been reported a TOF of 11 for the supported CoOx/zeolite [28]. Table 4 compares the efficiency of our catalysts with some found in the literature. All of these reports have lower TOF values than  $[\text{CoL}_1]^{2+}\text{-Y}$ ,  $[\text{CoL}_2]^{2+}\text{-Y}$  and  $[\text{CoL}_3]^{2+}\text{-Y}$  in the present research. So the comparison of epoxidation reaction time of our catalysts (2.5 h) with the other reports (3 h) [33, 34], (24 h) [32] and (5 h) [28, 35] is many considerable.

In summary we can conclude that three different Co(II) macrocyclic Schiff base complexes has been successfully encapsulated inside the cavity of zeolite Y and were well characterized. The resulting heterogeneous catalysts show high performance for epoxidation of alkenes. Encapsulated complexes are recyclable and retain a high level of catalytic activity during many cycles.

#### ACKNOWLEDGMENTS

The authors acknowledge the Damghan University for the support of this work.

**Table 3.** Epoxidation of cyclooctene with  $\text{O}_2$  using recycled catalysts. Reaction conditions: alkene (10 mmol), catalyst (20 mg),  $75^\circ\text{C}$ ,  $\text{CH}_3\text{CN}$  (15 mL),  $\text{O}_2$  (1 atm bubbling 15 mL/min) isobutyraldehyde (30 mmol)

Number of cycle	$[\text{CoL}_1]^{2+}\text{-Y}$		$[\text{CoL}_2]^{2+}\text{-Y}$		$[\text{CoL}_3]^{2+}\text{-Y}$	
	conversion, %	epoxide yield, %	conversion, %	epoxide yield, %	conversion, %	epoxide yield, %
1	94.5	97	98.2	97.9	92.8	97.2
2	93.3	96.2	97.3	96.3	91	96.1
3	92.4	95.5	96.5	95.7	90.2	95
4	91.1	94.6	95.6	94.8	89.4	93.7
5	89	93.5	94.4	94	88.3	92.4

**Table 4.** Epoxidation of cyclooctene with molecular oxygen catalyzed by a variety of cobalt catalysts

Catalyst	Conversion, %	Epoxide, %	TOF, $\text{h}^{-1}$	References
Co(II)-MCM-41	78	78	47	31
Co(II)-PSA	92	98	15.4	32
CoOx/4A	43.4	98.9	11	28
Co-ZSM-5(L <sub>1</sub> )	43	100	13.2	33
Co-ZSM-5(L <sub>2</sub> )	41.9	100	13	33
Co-ZSM-5(L <sub>3</sub> )	41.8	100	13	33
CoO-MCM-41	95	—	17.6	34
$[\text{CoL}_1]^{2+}\text{-Y}$	94.5	97	386	Present work
$[\text{CoL}_2]^{2+}\text{-Y}$	98.2	97.9	418	Present work
$[\text{CoL}_3]^{2+}\text{-Y}$	92.8	97.2	393	Present work

## REFERENCES

1. Talsi, E.P. and Bryliakov, K.P., *Coord. Chem. Rev.*, 2012, vol. 256, p. 1418.
2. Adam, W., Saha Moller, C.R., and Ganeshpure, P.A., *Chem. Rev.*, 2001, vol. 101, p. 3499.
3. Blaser, H.U., Pugin, B., and Spindler, F., *J. Mol. Catal., A*, 2005, vol. 231, p. 1.
4. Beller, M., *Adv. Synth. Catal.*, 2004, vol. 346, p. 107.
5. Silva, A.R., Budarin, V., Clark, J.H., et al., *Carbon*, 2005, vol. 43, p. 2096.
6. Jørgensen, K.A., *Chem. Rev.*, 1989, vol. 89, p. 431.
7. Hunter, R., Turner, P., and Rimmer, S., *Synth. Commun.*, 2000, vol. 30, p. 4461.
8. Sheldon, R.A. and Kochi, J.K., *Metal-Catalyzed Oxidation of Organic Compounds*, New York: Academic, 1981, p. 271.
9. Koola, J.D. and Kochi, J.K., *J. Org. Chem.*, 1987, vol. 52, p. 4545.
10. Zombeck, A., Hamilton, D., and Drago, R.S., *J. Am. Chem. Soc.*, 1982, vol. 104, p. 6782.
11. Hamilton, D.E., Drago, R.S., and Zombeck, A., *J. Am. Chem. Soc.*, 1987, vol. 109, p. 374.
12. Bezaatpour, A., Amiri, M., and Jahed, V., *J. Coord. Chem.*, 2011, vol. 64, p. 1837.
13. Salavati-Niasari, M., Salimi, Z., Bazarganipour, M., and Davar, F., *Inorg. Chim. Acta*, 2009, vol. 362, p. 3715.
14. Banaei, A. and Rezazadeh, B., *J. Coord. Chem.*, 2013, vol. 66, p. 2129.
15. Tas, E., Aslanoglu, M., Kilic, A., et al., *J. Chem. Res.*, 2006, vol. 4, p. 242.
16. Temel, H., Cakir, U., and Ugras, I.H., *Synt. React. Inorg. Met. Org. Chem.*, 2004, vol. 34, p. 819.
17. Corma, A. and Garcia, H., *Eur. J. Inorg. Chem.*, 2004, p. 1143.
18. Quayle, W.H. and Lunsford, J.H., *Inorg. Chem.*, 1982, vol. 21, p. 97.
19. Kumar, D.S. and Alexander, V., *Polyhedron*, 1999, vol. 18, p. 1561.
20. Salavati-Niasari, M., Davara, F., and Saberyan, K., *Polyhedron*, 2010, vol. 29, p. 2149.
21. Temel, H., Kilic, A., and Tas, E., *J. Coord. Chem.*, 2008, vol. 61, p. 1443.
22. Ilhan, S., Temel, H., Kilic, A., and Tas, E., *Transition, Met. Chem.*, 2007, vol. 32, p. 1012.
23. Diegruber, H., Plath, P.J., Schulz-Ekloff, G., and Mohl, M., *J. Mol. Catal.*, 1984, vol. 24, p. 115.
24. Salavati-Niasari, M., *J. Mol. Catal. A: Chem.*, 2008, vol. 283, p. 120.
25. Le, Z.G., Liu, Z., Qian, Y., and Wang, C., *Appl. Surf. Sci.*, 2012, vol. 258, p. 5348.
26. Saha, D., Maity, T., Bera, R., and Koner, S., *Polyhedron*, 2013, vol. 56, p. 30.
27. Li, Z., Wu, Sh., Ding, H., et al., *New J. Chem.*, 2013, vol. 37, p. 1561.
28. Ma, X.T., Lu, X.H., Wei, C.C., et al., *Catal. Commun.*, 2015, vol. 67, p. 98.
29. Bhadbhade, M.M. and Srinivas, D., *Inorg. Chem.*, 1993, vol. 32, p. 6122.
30. Deshpande, S., Srinivas, D., and Ratnasamy, P., *J. Catal.*, 1999, vol. 188, p. 261.
31. Rezazadeh, B., Pourali, A., Banaei, A., and Behniafar, H., *J. Coord. Chem.*, 2019, vol. 72, p. 3401.
32. Bhunia, S., Jana, S., Saha, D., et al., *Catal. Sci. Technol.*, 2014, vol. 4, p. 1820.
33. Kazemnejadi, M., Shakeri, A., Nikookar, M., et al., *Res. Chem. Intermed.*, 2017, vol. 43, p. 6889.
34. Dhar, D., Koltypin, Y., Gedanken, A., and Chandrasekaran, S., *Catal. Lett.*, 2003, vol. 86, p. 197.
35. Qi, B., Lu, X.H., Fang, S.Y., et al., *J. Mol. Catal. A*, 2011, vol. 334, p. 44.